



HAL
open science

Topology and Failure Modeling for Optical Network Resilience Analysis Against Earthquakes

Anuj Agrawal, Vimal Bhatia, Shashi Prakash

► **To cite this version:**

Anuj Agrawal, Vimal Bhatia, Shashi Prakash. Topology and Failure Modeling for Optical Network Resilience Analysis Against Earthquakes. 23th International IFIP Conference on Optical Network Design and Modeling (ONDM), May 2019, Athens, Greece. pp.584-597, 10.1007/978-3-030-38085-4_50 . hal-03200664

HAL Id: hal-03200664

<https://inria.hal.science/hal-03200664v1>

Submitted on 16 Apr 2021

HAL is a multi-disciplinary open access archive for the deposit and dissemination of scientific research documents, whether they are published or not. The documents may come from teaching and research institutions in France or abroad, or from public or private research centers.

L'archive ouverte pluridisciplinaire **HAL**, est destinée au dépôt et à la diffusion de documents scientifiques de niveau recherche, publiés ou non, émanant des établissements d'enseignement et de recherche français ou étrangers, des laboratoires publics ou privés.



Distributed under a Creative Commons Attribution 4.0 International License

Topology and Failure Modeling for Optical Network Resilience Analysis Against Earthquakes

Anuj Agrawal¹ (Student Member, IEEE, OSA),
Vimal Bhatia¹ (Senior Member, IEEE) and Shashi Prakash² (Senior Member, IEEE, OSA)

¹ Signals and Software Group, Discipline of Electrical Engineering, Indian Institute of Technology Indore, Indore 453552, India
{phd1501202003, vbhatia}@iiti.ac.in

² Photonics Laboratory, Devi Ahilya University, Indore, India 452017
sprakash@ietdavv.edu.in

Abstract. In this paper, we propose a stochastic failure and optical network topology (SFONT) model that can be used to comprehensively analyze the resilience of optical networks against a large number of possible earthquakes. We study an optical network densification problem, where dense network topologies are generated using the proposed SFONT model. Further, a seismic-risk aware optical network densification (SRA-OND) scheme is proposed with a view to design the future optical networks robust against earthquakes. The proposed SFONT model has been evaluated at various stages of network densification. To validate the capability of the proposed SFONT model to emulate real-world networking and failure scenario, we also perform a similar analysis based on RailTel optical network topology, seismic hazard maps, and real past earthquake data from India. Simulations indicate that the proposed SFONT model can be used to estimate and analyze the impact of network-resilience schemes on optical networks for a large number of possible earthquakes.

1 Introduction

Earthquakes have been a major cause of optical fiber cable (OFC) destruction in the past. For instance, the 2008 China Sichuan earthquake of magnitude 8.0 destroyed around 30,000 km of OFCs [1]. In a telecom-cloud infrastructure (TCI) supported by optical network, various nodes interconnect datacenters (DCs), multiprotocol label switching (MPLS) areas, and cable landing stations (CLS) through OFCs [2,3]. A rapid increase in the number of DC and OFC deployment has been observed in the recent past, and many more DCs and OFCs are planned to be deployed in future to enable beyond 5G telecommunication, and cloud services [4]. Moreover, to realize the maximum benefits of wireless network densification, backhaul optical networks also need to be densified [4,5]. Thus, with a view to make the future TCI resilient against earthquakes, the optical network components (nodes/links) should be physically located in the low seismic-risk regions.

To design robust future optical networks, a method for comprehensive and long-term analysis of various network-resilience schemes is required to assess optical networks against a large number of possible earthquakes. Thus, in this work, we propose a stochastic failure and optical network topology (SFONT) model that can be used to estimate and analyze the impact of various network-resilience schemes on optical networks.

Since large-scale natural disasters such as earthquakes affect a large geographical region, all the fiber cables lying in that region may fail simultaneously. Such a large-scale failure caused due to a common disaster occurrence is referred to as geographically correlated multi-link failure (GCMF). In the studies [1,6–9] that address the problem of robust

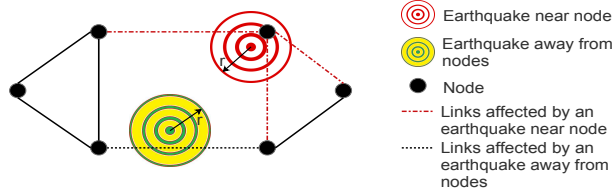


Fig. 1: Possibility of GCMFs in a mesh-connected optical network due to earthquakes at different epicenter locations around the network.

physical network design, most of the works propose physical fiber route modification as a solution to achieve network robustness. However, in Fig. 1, we show that GCMFs are highly dependent on the physical location of nodes.

In Fig. 1, an example mesh-connected 6-node optical network is shown. Here, two earthquakes causing disaster in a circular area of radius r from their epicenters are shown. It can be observed that the earthquake that occur in the vicinity of node is vulnerable to a GCMF affecting three fiber links. However, the earthquake that occur far away from nodes is vulnerable to single-link failure that can be survived using the conventional dedicated path protection (DPP), or shared path protection (SPP) methods. Thus, for resilient network design against GCMFs, the locations of nodes are of utmost concern. For simulations, we consider GCMFs caused due to earthquakes having epicenters in the vicinity of nodes.

In this work, we study an optical network densification (OND) scenario with a view to design the future dense optical networks resilient against earthquakes. We propose a seismic-risk aware optical network densification (SRA-OND) scheme for robust physical network topology design that finds the low seismic-risk regions to locate the new nodes. We evaluate the proposed SFONT model by analyzing various OND stages using the proposed SRA-OND as well as a seismic-risk unaware (SRU)-OND approach (where nodes are randomly located without considering seismic risk). To verify the capability of the proposed SFONT model to emulate real-world network topologies and failure scenarios, we compare the proposed SFONT model with a real-world case considering past real earthquakes [10], and real Indian RailTel optical network topology [11].

Related Work: The failure modeling and resilience analyses done by majority of the studies [6–8, 12–15] are based on one/two network topology, arbitrary disaster zones, and few instances of disaster occurrence. However, for a comprehensive and rigorous assessment of any resilience-improvement scheme, they should be analyzed for a number of randomly obtained networks, since the performance may vary with changes in network topologies. In the proposed SFONT model, random network topologies of varying size and connectivity are obtained in each iteration. In [8, 9], spatially uniform occurrence of disasters has been assumed in a given geographical region. However, practically, in a large geographical region, the probability of occurrence of natural disasters varies with different geographical locations. We incorporate this characteristic of spatially non-uniform disaster probability in the proposed SFONT model to generate earthquake epicenters. Moreover, we leverage the spatially non-uniform disaster probability in the proposed SRA-OND to locate the nodes in low seismic-risk regions. In [12], four arbitrary sample disaster zones have been assumed for resilience-analysis. Random disaster zones have been assumed in [14] without considering any disaster risk model. However, for a comprehensive and

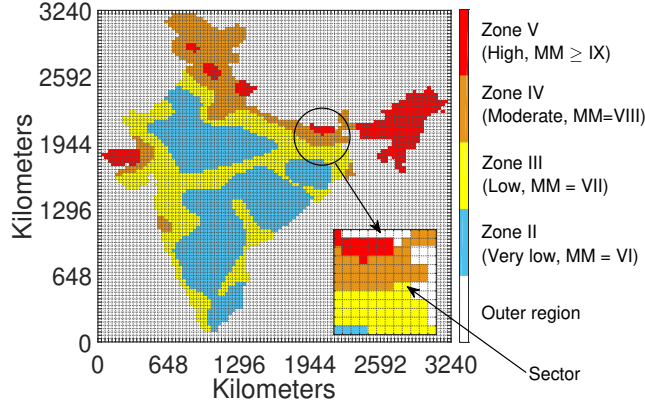


Fig. 2: Seismic Hazard map of India [16] subdivided into sectors.

long-term assessment of any resilience-improvement scheme, it should be tested for a large number of possible disaster occurrences.

For the first time in the literature, in the proposed SFONT model, we perform optical network densification in a given geographical region using Matérn hard core point process (MHCPP) and Gabriel graphs (GGs). To generate large number of spatially non-uniformly distributed earthquakes as per seismic-risk, we employ Poisson point process (PPP). The proposed SFONT model is described in the next section. The notations used in this paper are summarized in Table 1.

2 Proposed Stochastic Failure and Optical Network Topology (SFONT) Model

To obtain network topology, and to generate failures in a geographical region, we consider a bounded set $\mathbf{G} \subset \mathbb{R}^2$ representing the geographical region of interest. In this paper, we consider a bounded region \mathbf{G} of 3240 km \times 3240 km representing India and the neighboring regions. The region lying outside the border of India is included in a set ${}_{\mathbf{n}}\mathbf{G}$ representing non-feasible regions for node placement. The objective is to obtain random network topology within the Indian terrestrial region ($\mathbf{G} \cap {}_{\mathbf{n}}\mathbf{G}$), and to generate spatially non-uniformly distributed earthquakes as per the seismic-risk. To obtain seismic-risk information, we consider the seismic hazard map of India [16] (shown in Fig. 2), which is classified in to four types of zones on the basis of maximum Modified Mercalli (MM) intensity of seismic shaking. In this work, to describe the proposed SFONT model and to validate the hypothesis, we consider the seismic hazard map of India. However, the proposed model is generic in the sense that it can be used to obtain failures and network topologies in any geographical region, given its seismic hazard map.

It can be observed from seismic hazard maps of various countries/continents [10, 16] that seismicity does not change for small distances, and thus seismic-risk of a small local region can be considered as uniform throughout that region. We convert the geographical region \mathbf{G} provided as an input into a grid-structure, as shown in Fig. 2, where the grid contains square shaped bounded regions of small area, which we refer as ‘sectors’. The whole geographical region is subdivided into n number of sectors, where each sector of area ${}_{\mathbf{a}}|\mathbf{B}|$ represents a bounded region in \mathbb{R}^2 , and the seismic risk (i.e., seismic zone type) does not change within a sector. We obtain the locations and density of earthquake epicenters in each $\mathbf{B}_i \in \mathbf{B}$ using the poisson point process (PPP) [17]. As per the definition of

Table 1: Notations

| Symbol | Description |
|--|--|
| Φ | point process (PP) |
| $\mathbb{R}^1 = \mathbb{R}$ | field of real number |
| \mathbb{R}^n | n -dimensional Euclidean space |
| \mathbb{N} | set of natural numbers |
| \mathbb{E} | expectation |
| \mathbb{P} | probability |
| $\text{dist}(a, b)$ | Euclidean distance between points a and b , where $a, b \in \mathbb{R}^2$ |
| \mathbf{G} | a bounded set representing the geographical region of interest, $\mathbf{G} \subset \mathbb{R}^2$ |
| ${}_{\mathbf{n}}\mathbf{G}$ | set of bounded regions non-feasible for node placement, ${}_{\mathbf{n}}\mathbf{G} \subset \mathbb{R}^2$, ${}_{\mathbf{n}}\mathbf{G} \subset \mathbf{G}$, index g (here, \mathbf{n} is prescript) |
| \mathbf{B} | a bounded set representing the geographical region of sectors, $\mathbf{B} \subset \mathbf{G}$, $\mathbf{B} \subset \mathbb{R}^2$, index i (i.e., \mathbf{B}_i denotes the bounded region of i^{th} sector) |
| ${}_{\mathbf{a}} \mathbf{G} , {}_{\mathbf{a}} \mathbf{B} $ | area of bounded regions represented by set \mathbf{G}, \mathbf{H} , respectively (here, \mathbf{a} is prescript) |
| l_G | length of the area of \mathbf{G} |
| b_G | breadth of the area of \mathbf{G} |
| a_i | length of the edge of sector \mathbf{B}_i |
| $\Phi(\mathbf{B})$ | number of points of PP in a bounded set \mathbf{B} |
| S | set of types of seismic zones, index s |
| λ | density of poisson point process (PPP) |
| λ^s | density of poisson point process (PPP) for zone type s |
| λ_m | density of MHCPP |
| ${}_{\mathbf{a}} \mathbf{G} \lambda$ | mean number of points of PP in a bounded region \mathbf{G} |
| r_h | hard core parameter of MHCPP |
| \mathbf{X} | set of points denoting epicenter coordinates, $\mathbf{X} \subset \mathbb{R}^2$, $\mathbf{X} \subset \mathbb{G}$ |
| \mathbf{V} | set of points representing node locations in original topology, $\mathbf{V} \subset \mathbb{R}^2$, $\mathbf{V} \subset \mathbb{G}$ |
| \mathbf{V}' | set of points representing locations of nodes in the SRA-OND topology |
| V | set of nodes, index v , $V \subset \mathbb{N}$ |
| W | set of links, index w , $V \subset \mathbb{N}$ |
| D | set of link lengths, index w , $V \subset \mathbb{N}$ |
| D' | set of link lengths in the SRA-OND topology, index w , $V \subset \mathbb{N}$ |
| K | set of sectors, index k , $K \subset \mathbb{N}$ |
| K^s | sector of type s seismic zone |
| $K(v)$ | set of sectors to be searched for shifting of v^{th} node (V_v), $K(v) \subset K$, index p |
| $K(n)$ | set of sectors non-feasible for node placement, $K(n) \subset K$ |
| $K(r)_k$ | set of sectors used to calculate SR_k , $K(r)_k \subset K$ |
| SR_k | seismic-risk associated with sector K_k |
| Ω | set of weights assigned to each sector as per their seismic zone type, index k (more weight is assigned to higher seismic zones) |
| $\Omega(V)$ | set of weights of sectors in which nodes are located, index v |
| n | number of sectors in the region \mathbf{G} , $n = K $ |
| n_k^r | number of sectors on the either sides of sector K_k used to calculate SR_k of sector K_k |
| n_k^f | number of sectors on the either sides of sector K_k (having earthquake epicenter) where if a node is located, multi-link failure will occur |
| c_k | center of sector K_k |
| M | magnitude of earthquake (on moment magnitude scale) |

PPP Φ of density λ , the number of points (q) in the bounded set $\mathbf{B} \subset \mathbb{R}^2$ has a poisson distribution with mean ${}_{\mathbf{a}}|\mathbf{B}|\lambda$, i.e.,

$$\mathbb{P}(\Phi(\mathbf{B}) = q) = \exp(-{}_{\mathbf{a}}|\mathbf{B}|\lambda) \frac{({}_{\mathbf{a}}|\mathbf{B}|\lambda)^q}{q!}, \quad (1)$$

where the density λ is given by

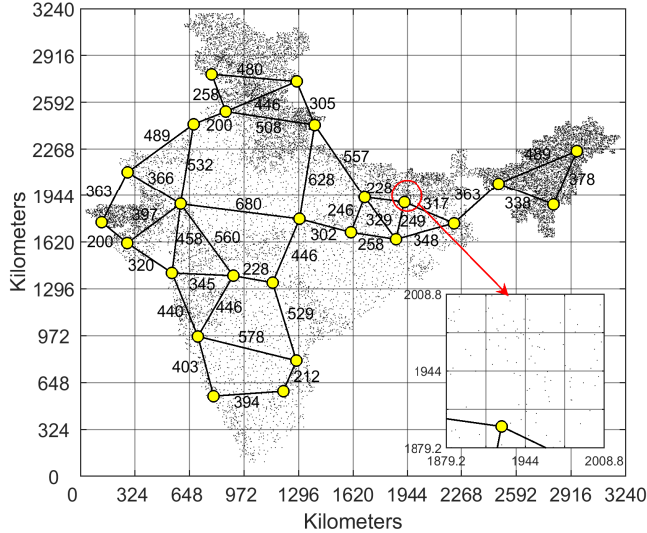


Fig. 3: Network topology and epicenters obtained using the proposed SFONT model. Link lengths are in km. (inset shows the epicenters obtained using PPP in different sectors).

$$\lambda = \frac{\mathbb{E}[\Phi(\mathbf{B})]}{a|\mathbf{B}|}. \quad (2)$$

In PPP, the number of points (epicenters) in a given bounded area is given by (1), and the location of points (\mathbf{X}) is uniformly distributed in each $\mathbf{B}_i \in \mathbf{B}$. Since earthquakes are more frequent in high seismic zones [10], we generate different number of earthquake epicenters using different values of density (λ^s), as given in Table 2. Large number of earthquake epicenters obtained in the given geographical region are shown in Fig. 3. It can be observed from Fig. 3 that the number of earthquakes per unit area decreases with seismic-risk in the order: Zone V \rightarrow Zone IV \rightarrow Zone III \rightarrow Zone II [16].

We consider significant earthquakes [10] ($M \geq 5$) for optical network resilience evaluation. To assign magnitude to the earthquake epicenters obtained in Fig. 3, we consider real statistics from the United States Geological Survey (USGS) [18], where the approximate percentage distribution of earthquakes of different range of magnitudes is: ($M \geq 8$) = 0.0624%; ($7 \leq M < 8$) = 0.8737%; ($6 \leq M < 7$) = 8.3717%; and ($5 \leq M < 6$) = 90.6922%. We denote the above ranges of magnitudes by M_{8+} , M_{7-8} , M_{6-7} , and M_{5-6} , respectively.

To design the physical network topology in the given geographical region, we generate random Gabriel graphs (GGs) [19, 20], modified by Matérn hard core point process (MHCPP) [17]. In the literature [19, 20], random GGs have been generated to design the network topologies, where a fixed number of nodes are located with uniform spatial distribution in a given geographical area. However, using uniform spatial distribution, it is possible that two or more nodes may get placed in the same location, which is impractical. Hence, we modify the GGs by MHCPP, that eliminates the impractical probability of two or more nodes being located at the same location, or very close to each other.

MHCPP is obtained from PPP, where points are first generated using PPP [17]. Then, some of the points are deleted such that no two points (nodes) with a separation less than r_h coexist in the constructed MHCPP. An instance of the proposed SFONT model

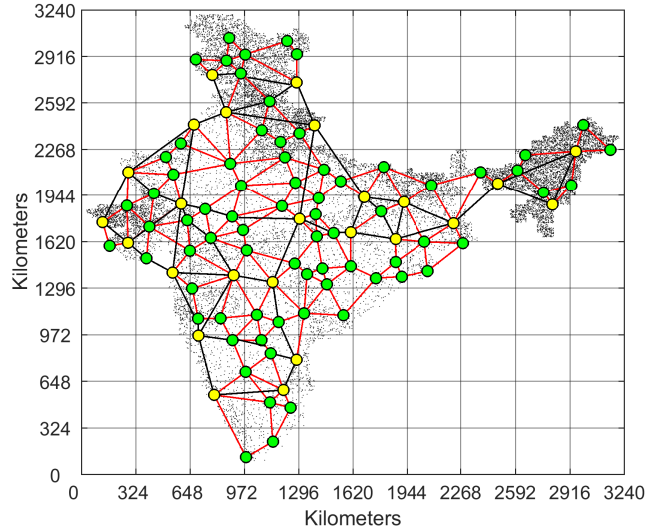


Fig. 4: Seismic risk unaware optical network densification (SRU-OND) of the network topology shown in Fig. 3. Here, the nodes of existing/initial network are represented by yellow color, and the new nodes (initially placed in the center of the desired region) to be deployed for network densification are shown in green color.

Table 2: Parameters values used to obtain earthquake epicenters in Fig. 2-3

| Parameter | Value |
|---|----------------------|
| Dimensions of bounded region \mathbf{G} , l_G, b_G | 3240 km |
| Length of edge of sectors $\mathbf{H} \subset \mathbf{G}$, a_h | 32.4 km |
| Set of types of seismic zones, S | $\{II, III, IV, V\}$ |
| PPP density for K^V , λ^V | 0.02 |
| PPP density for K^{IV} , λ^{IV} | 0.01 |
| PPP density for K^{III} , λ^{III} | 0.004 |
| PPP density for K^{II} , λ^{II} | 0.001 |
| Range of M for K^V , | $[5, 10)$ |
| Range of M for K^{IV} , | $[5, 8)$ |
| Range of M for K^{III} , | $[5, 7)$ |
| Range of M for K^{II} , | $[5, 7)$ |
| Hard core parameter, r_h | 200 km |

is shown in Fig. 3, where $r_h = 200$ km, and $|\mathbf{G}| \lambda_m = 25$. It can be seen from Fig. 3 that there is at least a distance of r_h km amongst different nodes. The fiber-links amongst various node-pairs are considered to be of shortest physical route. To rigorously assess various network-resilience schemes for physical network design, logical topology design, protection, restoration, early warning data backup, survivable routing, etc., networks of different size and topology can be obtained by tuning different parameters, and evaluated for a large number of possible failures using the proposed SFONT model.

3 Proposed Seismic Risk Aware Optical Network Densification (SRA-OND) Scheme

The proposed SRA-OND scheme can be used to perform OND so as to make the future TCI robust against earthquake induced GCMFs. We assume that the desired region for

each new node to be deployed is a square area of size 5×5 sectors. The randomly obtained node locations in the proposed SFONT model are assumed as the center of the desired regions for node deployment. Node shifting is then performed to calculate the seismic-risk (SR) for all the nodes to be placed within their desired regions. In the proposed SRA-OND, a bounded geographical region $\mathbf{G} \subset \mathbb{R}^2$ (square or rectangular) subdivided into sectors \mathbf{B} , and a network topology with locations of all the nodes, are provided as input. The current locations \mathbf{V} of all the nodes are also provided as input. The proposed SRA-OND is described in the following steps as follows:

Step 1: The set of non-feasible sectors $K(n)$ is found, where all the sectors having a common region to that specified in \mathbf{nG} , are included in the set $K(n)$.

Step 2: For each $V_v \in V$, node shifting is performed from the current (i.e., central) sector to all other sectors lying within the desired region (of size 5×5 sectors) for node deployment.

Step 3: The SR_k corresponding to each sector K_k is calculated. The SR_k for k^{th} sector is calculated using the seismic zone type of nearby n_k^r sectors, and the Euclidean distance of these sectors from the k^{th} sector. We calculate SR_k using (3) as

$$SR_k = \sum \Omega_k \cdot \mathbf{dist}(c_k, c_l), \forall K_l \in K(r)_k, \quad (3)$$

where, c_l represents the center of sectors in $K(r)_k$.

Step 4: Amongst all the sectors in $K(v)$ for the node $V_v \in V$, the sector with minimum value of SR_k is chosen for node placement (provided a sector of lower seismic zone type is found in the desired region).

Step 5: The modified node locations (\mathbf{V}'), and link distances (\mathbf{D}') are returned by the proposed SRA-OND scheme.

4 Performance Evaluation

In this section, resilience-evaluation of network topologies has been performed considering network densification in various stages. We consider four stages of network densification, namely, Stage 1 (S_1), Stage 2 (S_2), Stage 3 (S_3), and Stage 4 (S_4). At each stage, the number of nodes is gradually increased by varying the value of λ_m . We generate 100 instances of the proposed SFONT model for the parameter values given in Table 2, except r_h , which is considered as 180 km, 150 km, 120 km, and 100 km for S_1 , S_2 , S_3 , and S_4 , respectively. The decreasing values of r_h indicate the decrease in minimum link-length with increased network densification. The effect of generated earthquakes on various random network topologies is then calculated.

To compare the proposed SRA-OND, we study another scheme, namely, SRU-OND, where network densification is seismic-risk unaware (SRU). To realize SRU-OND, the nodes have been located in the central sector of the desired regions for each node to be deployed. To evaluate the proposed SRA-OND scheme under real-world network scenario, all the significant past earthquakes that occurred since the year 1900 in India [10] have been simulated. We use the Richter logarithmic scale to generate GCMFs based on the distance between epicenter and node [21]. Accordingly, we use the distance ratio $n_k^f : 3n_k^f : 6n_k^f : 10n_k^f$ to generate GCMFs due to various earthquakes of magnitude M_{5-6} , M_{6-7} , M_{7-8} , and M_{8+} , respectively. The average number of nodes corresponding to S_1 , S_2 , S_3 , and S_4 are ${}_a|\mathbf{G}|\lambda_m = 40$, ${}_a|\mathbf{G}|\lambda_m = 60$, ${}_a|\mathbf{G}|\lambda_m = 80$, and ${}_a|\mathbf{G}|\lambda_m = 100$, which shows gradual network densification.

Fig. 3 shows the initial network topology (which represents the existing network to be densified) obtained using the proposed SFONT model, and Fig. 4 shows the dense

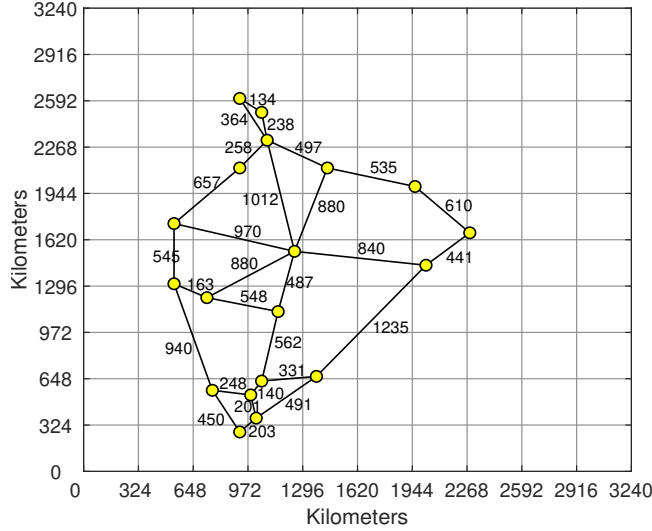


Fig. 5: 19-node RailTel network topology [11]. Link lengths are in km.

network obtained at S_4 by adding nodes in the initial topology shown in Fig. 3. The 19-node RailTel network topology is shown in Fig. 5, and the dense network at S_4 for the topology shown in Fig. 5 is shown in Fig. 6. The SRA-OND topology corresponding to Fig. 6 is shown in Fig. 7, where the nodes interconnected by blue solid lines represent the SRA-OND topology obtained by seismic-risk aware node shifting, whereas the initial randomly obtained nodes interconnected by black dashed lines represent the part of SRU-OND topology which has been modified in the SRA-OND topology. Here, the nodes which are either already located in the lowest seismic zone, or could not be relocated in a lower seismic zone within the desired region (of size 5×5 sectors) for that node are kept at their original locations. Similar to Fig. 7, SRA-OND is performed for each of the 100 generated instances of the proposed SFONT model.

We perform routing, modulation, and spectrum allocation (RMSA) for each request in a set of 1000 randomly generated connection requests (in each topology) having heterogeneous bandwidth requirements uniformly selected from the set $\{40, 200, 500, 1000\}$ Gbps. We perform distance adaptive modulation, first-fit spectrum allocation, and k -shortest paths routing. After establishing all the requests, the spectrum state is frozen, and the effect of earthquakes is obtained (using $n_k^f = 1$) in terms of cumulative bandwidth loss (BL) in Tbps, and connection drop ratio (CDR). CDR is defined as the ratio of the number of connections dropped due to earthquake to the number of connections established before the earthquake arrival.

Fig. 8-11 show the simulation results in terms of BL and CDR . In Fig. 8, BL due to a large number of earthquakes (18000) generated using the proposed SFONT model is shown. Simulations at the first (S_1) and the fourth (S_4) stage of network densification are shown to compare the proposed SRA-OND with the SRU-OND. It can be observed from Fig. 8 that at both the S_1 and S_4 stages, significant reduction in BL due to earthquakes has been achieved. An average reduction of 14.3%, and 29.9% in BL at S_1 , and S_4 , respectively, has been achieved using the proposed SRA-OND, which demonstrates the advantage of seismic-risk aware physical network design. Besides, it is observed that with

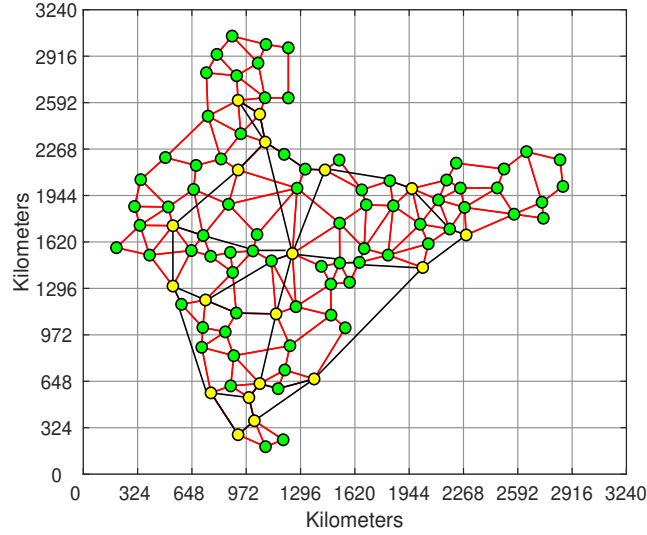


Fig. 6: Seismic risk unaware optical network densification (SRU-OND) of the 19-node RailTel network topology shown in Fig. 5. Here, the nodes of 19-node RailTel network are represented by yellow color, and the new nodes (initially placed in the center of the desired region) to be deployed for network densification are shown in green color.

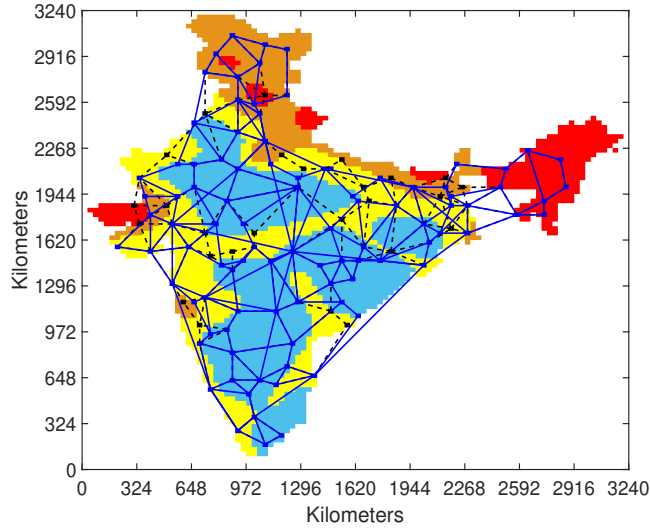


Fig. 7: Seismic risk aware optical network densification (SRA-OND) of the 19-node RailTel network topology (here, the location of new nodes are identified as the sector with minimum seismic risk (SR_k) within the desired region of node placement)

increased network densification, the improvement in BL using the proposed SRA-OND increases, which shows the long-term advantage of the proposed SRA-OND scheme.

Fig. 9 shows the BL obtained due to the 87 past earthquakes occurred since the year 1900 in India at different locations. The initial topology considered in this case is the 19-node Indian RailTel network topology [11]. The earthquakes have been simulated randomly from the set of 87 earthquakes at each of the 100 iterations for every densification stage. Simulation results obtained in Fig. 9 show a similar trend with that obtained

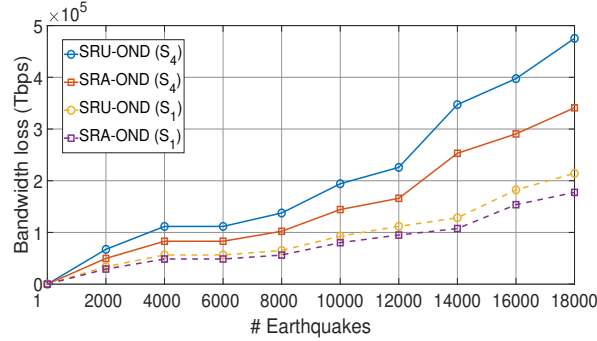


Fig. 8: Cumulative bandwidth loss (BL) due to earthquakes for SRU-OND and SRA-OND under the proposed SFONT model.

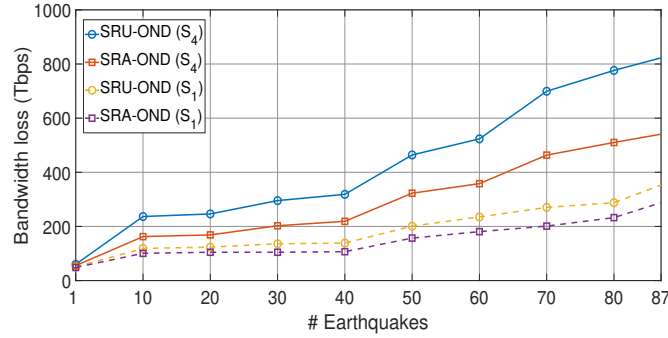


Fig. 9: Cumulative bandwidth loss (BL) due to past real earthquakes for SRU-OND and SRA-OND of 19-node RailTel network.

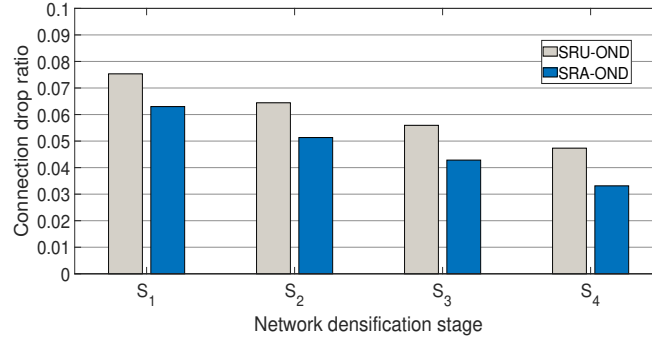


Fig. 10: Connection drop ratio (CDR) for SRU-OND and SRA-OND under the proposed SFONT model at different network densification stages.

under the proposed SFONT model in Fig. 8. As the size of earthquake data set is smaller in Fig. 9, the amount of BL is also smaller as compared to that in Fig. 8. However, the average improvement in BL using the proposed SRA-OND is 17.1% and 38.2% at S_1 and S_4 , respectively, which highlights the advantage of considering seismic-risk while densifying optical networks.

In Fig. 10-11, CDR has been evaluated at S_1 , S_2 , S_3 , and S_4 after simulating all the earthquakes. In Fig. 10, CDR under the proposed SFONT model has been evaluated. It is observed from Fig. 10 that CDR decreases with increased network densification, since the

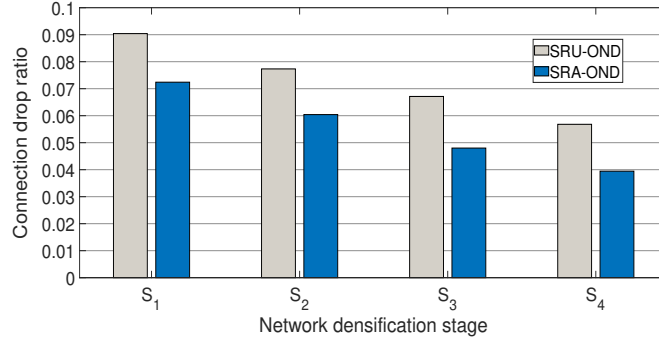


Fig. 11: Connection drop ratio (CDR) for SRU-OND and SRA-OND of the 19-node RailTel network at different network densification stages.

percentage amount of traffic per unit node/link decreases with network densification (i.e., the number of connections dropped per unit node/link-failure decreases with network densification). It is also observed that at all the four stages, the proposed SRA-OND performs better than the SRU-OND. In Fig. 11, CDR for past real earthquakes in India for densification of 19-node RailTel network has been evaluated, where a similar trend of results has been observed as that obtained under the proposed SFONT model in Fig. 10.

The similarity observed in the trend of results obtained under the proposed SFONT model and that obtained for the RailTel network densification and real past earthquakes show that the proposed SFONT model can be used to emulate earthquake failures and network topologies, given the seismic hazard map any region. Thus, the proposed SFONT model can be used to estimate the impact of various network-resilience schemes on optical networks for a large number of possible earthquakes.

5 Conclusion

We proposed an SFONT model using PPP, MHCPP, and GGs that can be used to comprehensively evaluate various network-resilience schemes for optical networks. Further, we proposed an SRA-OND scheme that can significantly reduce the BL due to earthquake induced GCMFs. The proposed SRA-OND scheme has been evaluated and compared with the SRU-OND scheme under the proposed SFONT model as well as for a real-world case from India. The similarity observed in the trend of results obtained under both the cases validates the capability of the proposed SFONT model to emulate real-world networks and failure scenarios. In future, we plan to design resilient DC interconnection network with a content-centric approach.

Acknowledgment

This publication is an outcome of the R&D work under the Visvesvaraya Ph.D. Scheme of the Ministry of Electronics & Information Technology (MeitY), Government of India (GoI), being implemented by Digital India Corporation. The authors would like to thank the Indian Institute of Technology (IIT) Indore for all the support and resources.

References

1. P. Tran and H. Saito, "Enhancing physical network robustness against earthquake disasters with additional links," *J. Lightw. Technol.*, vol. 34, no. 22, pp. 5226–5238, 2016.
2. L. Velasco and M. Ruiz, *Provisioning, Recovery, and In-Operation Planning in Elastic Optical Networks*. John Wiley & Sons, 2017.

3. Ciena webinar: Diving into the Data Center Interconnect (DCI) Seascape [Online]. Available: <https://mynetwork.ciena.com/webinar-diving-into-the-dci-seascape-tyou.html?aliId=54469151>.
4. Ciena webinar: 5G will need fiber and lots of it [Online]. Available: <http://www.ciena.com/insights/webinars/5G-Will-Need-Fiber-and-Lots-of-It.html>.
5. N. Bhushan, J. Li, D. Malladi, R. Gilmore, D. Brenner, A. Damnjanovic, R. T. Sukhavasi, C. Patel, and S. Geirhofer, "Network densification: the dominant theme for wireless evolution into 5G," *IEEE Commun. Mag.*, vol. 52, no. 2, pp. 82–89, 2014.
6. P. N. Tran and H. Saito, "Geographical route design of physical networks using earthquake risk information," *IEEE Commun. Mag.*, vol. 54, no. 7, pp. 131–137, 2016.
7. D. L. Msongaleli, F. Dikbiyik, M. Zukerman, and B. Mukherjee, "Disaster-aware submarine fiber-optic cable deployment for mesh networks," *J. Lightw. Technol.*, vol. 34, no. 18, pp. 4293–4303, 2016.
8. H. Saito, "Spatial design of physical network robust against earthquakes," *J. Lightw. Technol.*, vol. 33, no. 2, pp. 443–458, 2015.
9. C. Cao, M. Zukerman, W. Wu, J. H. Manton, and B. Moran, "Survivable topology design of submarine networks," *J. Lightw. Technol.*, vol. 31, no. 5, pp. 715–730, 2013.
10. USGS Search Earthquake Catalog [Online]. Available: <https://earth-quake.usgs.gov/earthquakes/search>.
11. R. J. Pandya, V. Chandra, and D. Chadha, "Simultaneous optimization of power economy and impairment awareness by traffic grooming, mixed regeneration, and all optical wavelength conversion with an experimental demonstration," *J. Lightw. Technol.*, vol. 32, no. 24, pp. 4166–4177, 2014.
12. N. H. Bao, M. Tornatore, C. U. Martel, and B. Mukherjee, "Fairness-aware degradation based multipath re-provisioning strategy for post-disaster telecom mesh networks," *J. Opt. Commun. Netw.*, vol. 8, no. 6, pp. 441–450, 2016.
13. A. Agrawal, U. Vyas, V. Bhatia, and S. Prakash, "SLA-aware differentiated QoS in elastic optical networks," *Opt. Fiber Technol.*, vol. 36, pp. 41–50, 2017.
14. M. F. Habib, M. Tornatore, M. De Leenheer, F. Dikbiyik, and B. Mukherjee, "Design of disaster-resilient optical datacenter networks," *J. Lightw. Technol.*, vol. 30, no. 16, pp. 2563–2573, 2012.
15. A. Agrawal, P. Sharma, V. Bhatia, and S. Prakash, "Survivability enhancement of backbone optical networks leveraging seismic zone information," in *Proc. IEEE Advanced Netw. and Telecommun. Sys. (ANTS)*, 2017, pp. 1–6.
16. C. V. R. Murty, Where are the seismic zones in India? [Online]. Available: <http://www.iitk.ac.in/nicee/EQTips/EQTip04.pdf>.
17. H. ElSawy, E. Hossain, and M. Haenggi, "Stochastic geometry for modeling, analysis, and design of multi-tier and cognitive cellular wireless networks: A survey," *IEEE Commun. Surv. Tut.*, vol. 15, no. 3, pp. 996–1019, 2013.
18. Earthquake Statistics, USGS [Online]. Available: <https://earthquake.us-gs.gov/earthquakes/browse/stats.php>.
19. I. Szcześniak, A. Gola, A. Jajszczyk, A. R. Pach, and B. Woźna-Szcześniak, "Itinerant routing in elastic optical networks," *J. Lightw. Technol.*, vol. 35, no. 10, pp. 1868–1875, 2017.
20. E. K. Cetinkaya, M. J. Alenazi, Y. Cheng, A. M. Peck, and J. P. Sterbenz, "On the fitness of geographic graph generators for modelling physical level topologies," in *Proc. Reliable Networks Design and Modeling (RNDM)*, Almaty, Kazakhstan, 2013, pp. 38–45.
21. C. J. Ammon, Earthquake Size [Online]. Available: http://eqseis.geosc.psu.edu/~cammon/HTML/Classes/IntroQuakes/Notes/earthquake_size.html.